

# Cross-correlating the EMU Pilot Survey I with CMB lensing: Constraints on cosmology and galaxy bias with harmonic-space power spectra



*University of Oxford*

Konstantinos Tanidis

In collaboration with J.Asorey, C.S.Saraf, C.Hale, B.Bahr-Kalus, D.Parkinson, S.Camera, R.P.Norris, A.M.Hopkins, M.Bilicki, N.Gupta

**CASTLE Tagliolo Monferrato**

**September 18th 2024**

# EMU Pilot Survey I

- Using ASKAP at 944MHz, covering a contiguous patch of  $\sim 270$  sq.deg, at a depth of 25-30  $\mu\text{Jy}/\text{beam}$  rms and with spatial resolution of 11-18 arcsec
- By the end of EMU, 70 million galaxies will be detected in the whole southern sky covered up to  $+30$  deg. in declination. The total sky coverage will be  $\sim 30,000$  sq.deg, ideal for ultra large-scale cosmology (relativistic effects and primordial Non-Gaussianity)

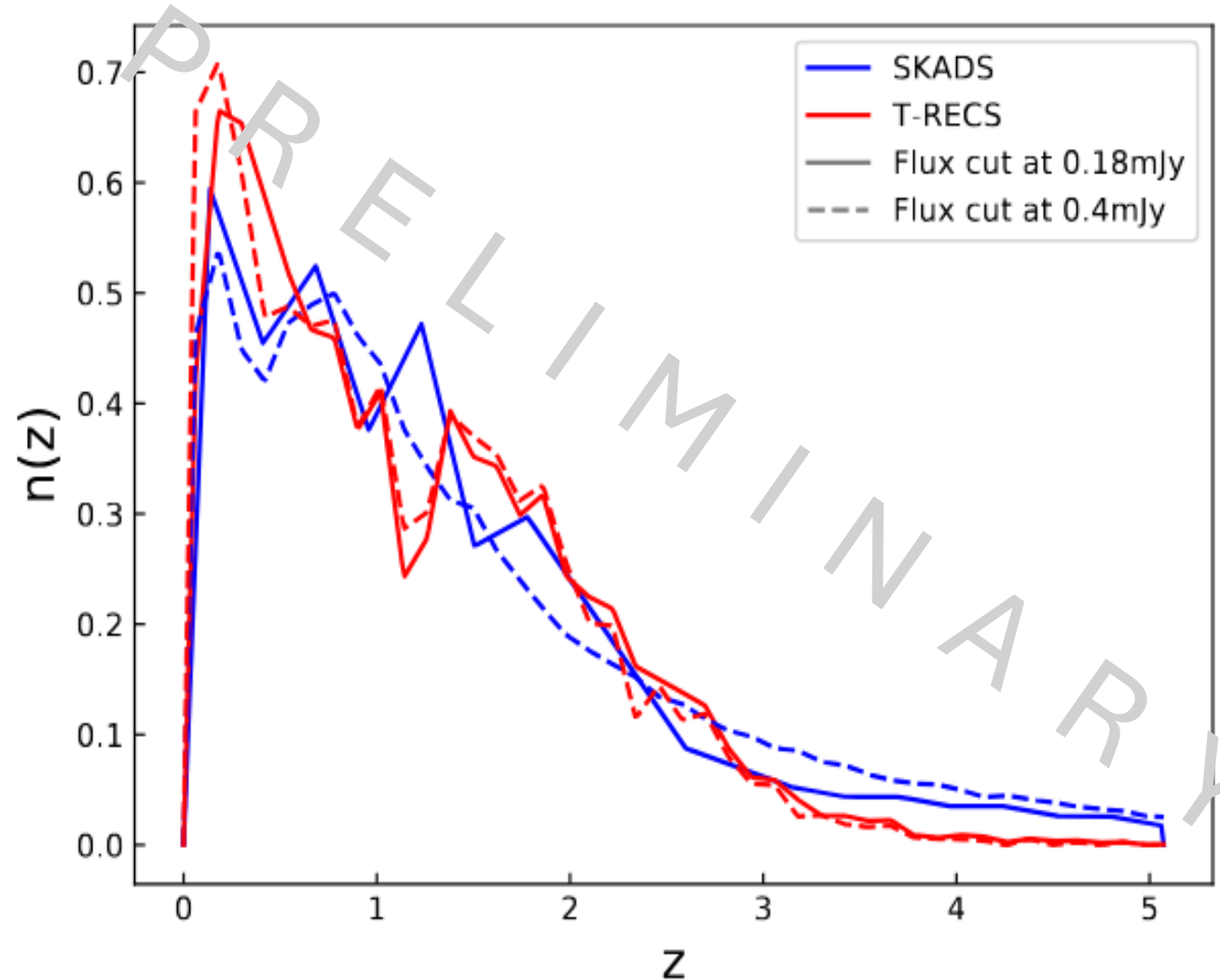


# EMU Pilot Survey I

- Radio continuum surveys use the synchrotron radiation as the galaxy tracer to scan quickly large patches of the sky thanks to the large field of view of the modern interferometers  
(EMU has  $\sim 30$ sq.deg)

# EMU Pilot Survey I

- Radio continuum surveys use the synchrotron radiation as the galaxy tracer to scan quickly large patches of the sky thanks to the large field of view of the modern interferometers (EMU has  $\sim 30\text{sq.deg}$ )
- Featureless, smooth power-law spectrum, w/o sharp features; redshift information unfeasible leading to large uncertainties on the redshift distribution of galaxy sample and its properties like the galaxy bias and halo mass
- Radio galaxy populations: AGN and SFG



# Limber approximated harmonic-space power spectra

$$S_{\ell, \text{th}}^{XY} = \int \frac{d\chi}{\chi^2} W^X(\ell, \chi) W^Y(\ell, \chi) P_{mm} \left( k = \frac{\ell + 1/2}{\chi}, \chi \right)$$

# Limber approximated harmonic-space power spectra

$$S_{\ell, \text{th}}^{XY} = \int \frac{d\chi}{\chi^2} W^X(\ell, \chi) W^Y(\ell, \chi) P_{mm} \left( k = \frac{\ell + 1/2}{\chi}, \chi \right)$$

**Galaxy number counts:**

$$\delta_g(\hat{n}) = \int b(\chi) n(\chi) \delta_m(z(\chi), \chi \hat{n})$$

$$W^{\delta_g}(\ell, \chi) \equiv W^{\delta_g}(\chi) = n(\chi) b(\chi)$$

# CMB Lensing

- The convergence field is the distortion of the CMB photon trajectories due to the gravitational potential caused by the underlying dark matter field

# CMB Lensing

- The convergence field is the distortion of the CMB photon trajectories due to the gravitational potential caused by the underlying dark matter field
- Unbiased tracer sensitive to the inhomogeneities of the matter field at high redshifts (peaks at  $z \sim 2$ )



# CMB Lensing

- The convergence field is the distortion of the CMB photon trajectories due to the gravitational potential caused by the underlying dark matter field
- Unbiased tracer sensitive to the inhomogeneities of the matter field at high redshifts (peaks at  $z \sim 2$ )
- Comparable volume with high- $z$  radio galaxies; ideal for cross-correlation with radio continuum galaxies

# CMB Lensing

- The convergence field is the distortion of the CMB photon trajectories due to the gravitational potential caused by the underlying dark matter field
- Unbiased tracer sensitive to the inhomogeneities of the matter field at high redshifts (peaks at  $z \sim 2$ )
- Comparable volume with high- $z$  radio galaxies; ideal for cross-correlation with radio continuum galaxies
  - Lifts degeneracy between the galaxy bias and the amplitude of the matter fluctuations

# Limber approximated harmonic-space power spectra

$$S_{\ell, \text{th}}^{XY} = \int \frac{d\chi}{\chi^2} W^X(\ell, \chi) W^Y(\ell, \chi) P_{mm} \left( k = \frac{\ell + 1/2}{\chi}, \chi \right)$$

**Convergence:**

$$\kappa(\hat{n}) = \int_0^{\chi^*} d\chi \frac{3\Omega_{m,0}H_0^2}{2c^2} [1 + z(\chi)] \chi \frac{\chi^* - \chi}{\chi^*} \delta_m(z(\chi), \chi \hat{n})$$

$$W^\kappa(\ell, \chi) = L(\ell) \frac{3\Omega_m H_0^2}{2c^2} [1 + z(\chi)] \chi \frac{\chi^* - \chi}{\chi^*}$$

$$L(\ell) = \frac{\ell(\ell + 1)}{(\ell + 1/2)^2}$$

# Detection algorithms

- Radio galaxies are large `blobs` that contain smaller (sub-)structures which can be part of the same galaxy (multi-components) or belong to a different one

# Detection algorithms

- Radio galaxies are large `blobs` that contain smaller (sub-)structures which can be part of the same galaxy (multi-components) or belong to a different one
  - Selavy island catalogue: Categorises large structures as single objects

# Detection algorithms

- Radio galaxies are large `blobs` that contain smaller (sub-)structures which can be part of the same galaxy (multi-components) or belong to a different one
  - Selavy island catalogue: Categorises large structures as single objects
    - PyBDSF: Categorises smaller structures as different objects

# Detection algorithms

- Radio galaxies are large `blobs` that contain smaller (sub-)structures which can be part of the same galaxy (multi-components) or belong to a different one
- Selavy island catalogue: Categorises large structures as single objects
  - PyBDSF: Categorises smaller structures as different objects
    - Apply two flux cuts:
      - 0.18mJy: 166,801 and 188,034 objects
      - 0.4mJy: 83,222 and 89,320 objects

- **Overdensity**

$$\delta_g(\hat{n}) = \frac{N_g(\hat{n})}{\bar{N}_g w_g(\hat{n})} - 1$$

$$\bar{N}_g = \langle N_g(\hat{n}) \rangle_n / \langle w_g(\hat{n}) \rangle_n$$

Set to 0 pixels with

$$w_g(\hat{n}) < 0.5.$$



# Maps

- Overdensity

$$\delta_g(\hat{n}) = \frac{N_g(\hat{n})}{\bar{N}_g w_g(\hat{n})} - 1$$

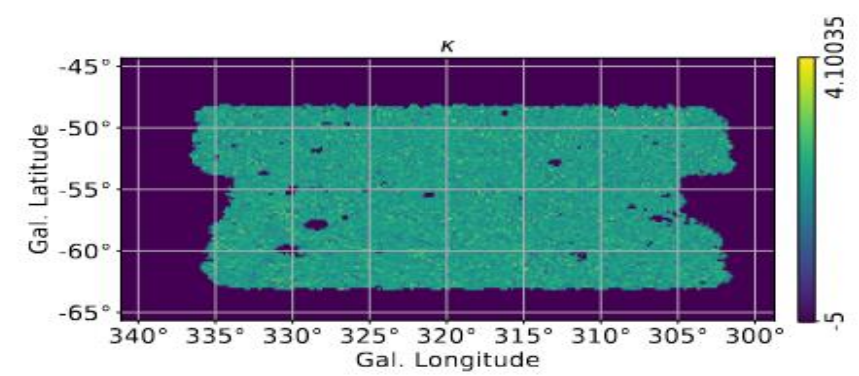
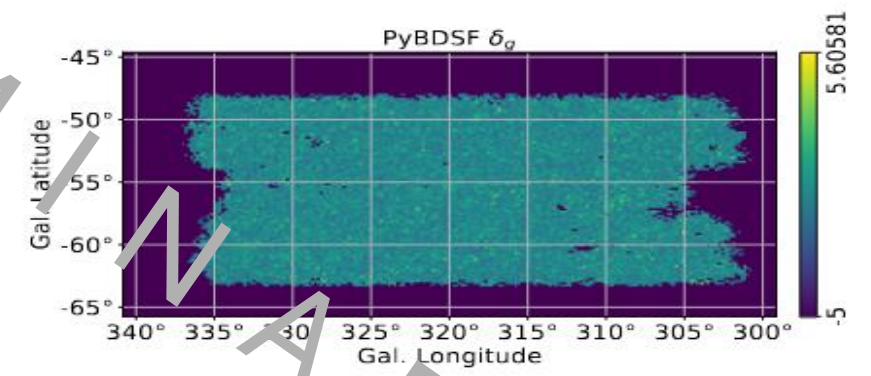
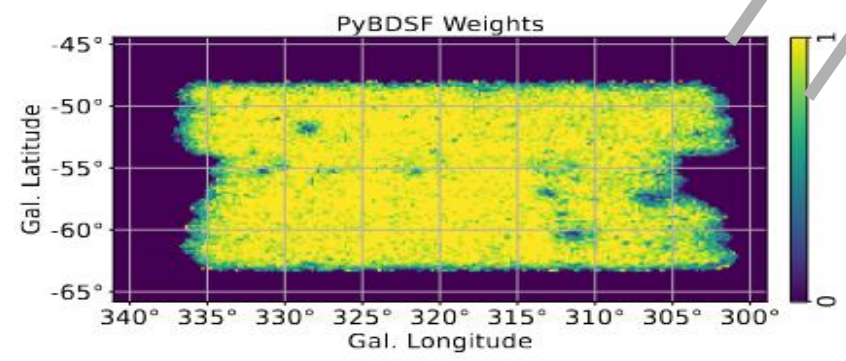
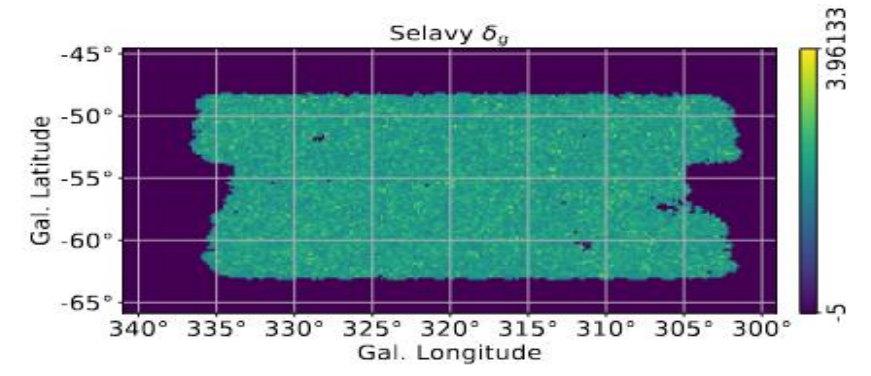
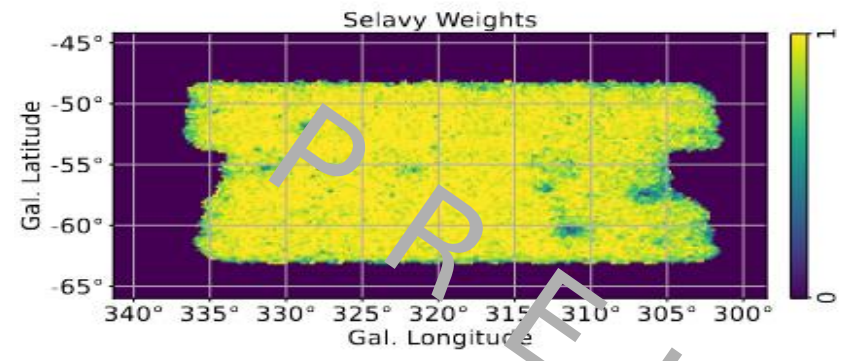
$$\bar{N}_g \equiv \langle N_g(\hat{n}) \rangle_n / \langle w_g(\hat{n}) \rangle_n$$

Set to 0 pixels with

$$w_g(\hat{n}) < 0.5.$$

- Planck PR4 convergence data

- Calculate pseudo-Cls accounting for the effect of the masks



# Gaussian covariance and log-likelihood

$$\text{Cov} = \begin{bmatrix} \text{Cov}^{gg,gg} & \text{Cov}^{gg,g\kappa} \\ (\text{Cov}^{gg,g\kappa})^T & \text{Cov}^{g\kappa,g\kappa} \end{bmatrix}$$

$$\text{Cov}_{\ell\ell'}^{gX,gY} = \frac{\delta_{\ell\ell'}}{(2\ell+1)\Delta\ell f_{\text{sky}}^{gX,gY}} [(\tilde{C}_{\ell}^{gg} + N_{\ell}^{gg})(\tilde{C}_{\ell'}^{XY} + N_{\ell'}^{XY}) + (\tilde{C}_{\ell}^{gX} + N_{\ell}^{gX})(\tilde{C}_{\ell'}^{gY} + N_{\ell'}^{gY})],$$

$$f_{\text{sky}}^{gX,gY} = \sqrt{f_{\text{sky}}^{gX} \cdot f_{\text{sky}}^{gY}}; \quad f_{\text{sky}}^{gg} \approx f_{\text{sky}}^{g\kappa}.$$

$$\chi^2(\mathbf{q}) = \sum_{\ell,\ell'} [d_{\ell} - t_{\ell}(\mathbf{q})]^T \text{Cov}_{\ell\ell'}^{-1} [d_{\ell} - t_{\ell}(\mathbf{q})]$$

$$\mathbf{d}_{\ell} = \{\tilde{C}_{\ell}^{gg}, \tilde{C}_{\ell}^{g\kappa}\} \text{ and } \mathbf{t}_{\ell} = \{\tilde{S}_{\ell}^{gg}, \tilde{S}_{\ell}^{g\kappa}\}$$

# Methodology

- Assume both a linear and a HALOFIT matter power spectrum

# Methodology

- Assume both a linear and a HALOFIT matter power spectrum
- Consider two different galaxy bias models: a constant bias  $b(z)=b_g$  ; and a constant amplitude  $b(z)=b_g/D(z)$ , with  $D(z)$  the linear growth factor

# Methodology

- Assume both a linear and a HALOFIT matter power spectrum
- Consider two different galaxy bias models: a constant bias  $b(z)=b_g$  ; and a constant amplitude  $b(z)=b_g/D(z)$ , with  $D(z)$  the linear growth factor
- Assume the analytic Gaussian covariance in the log-likelihood

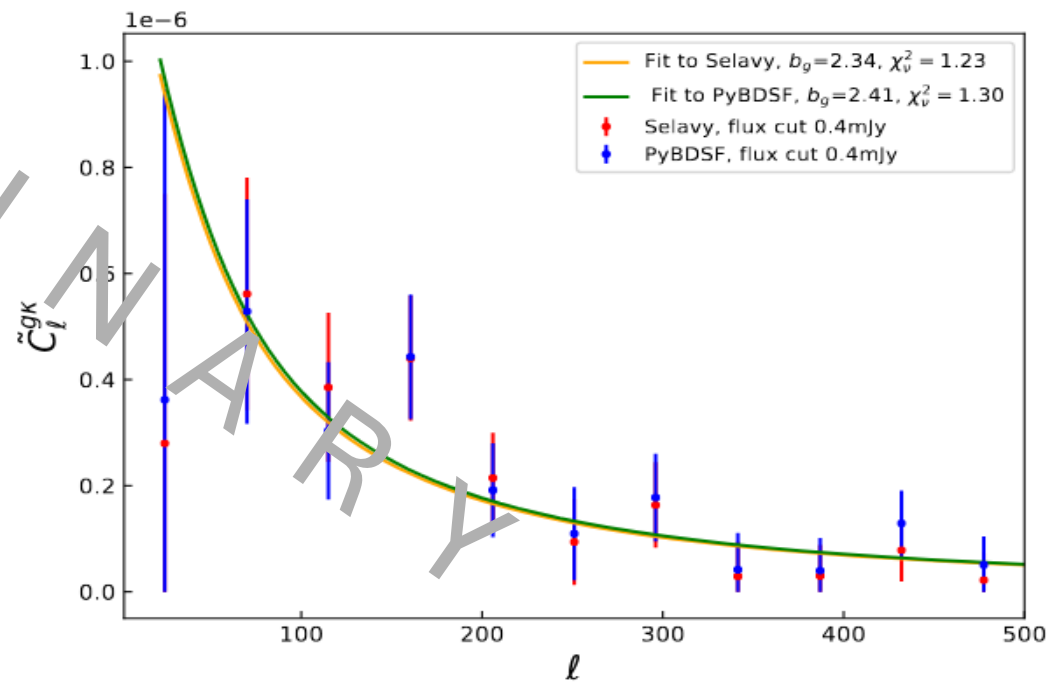
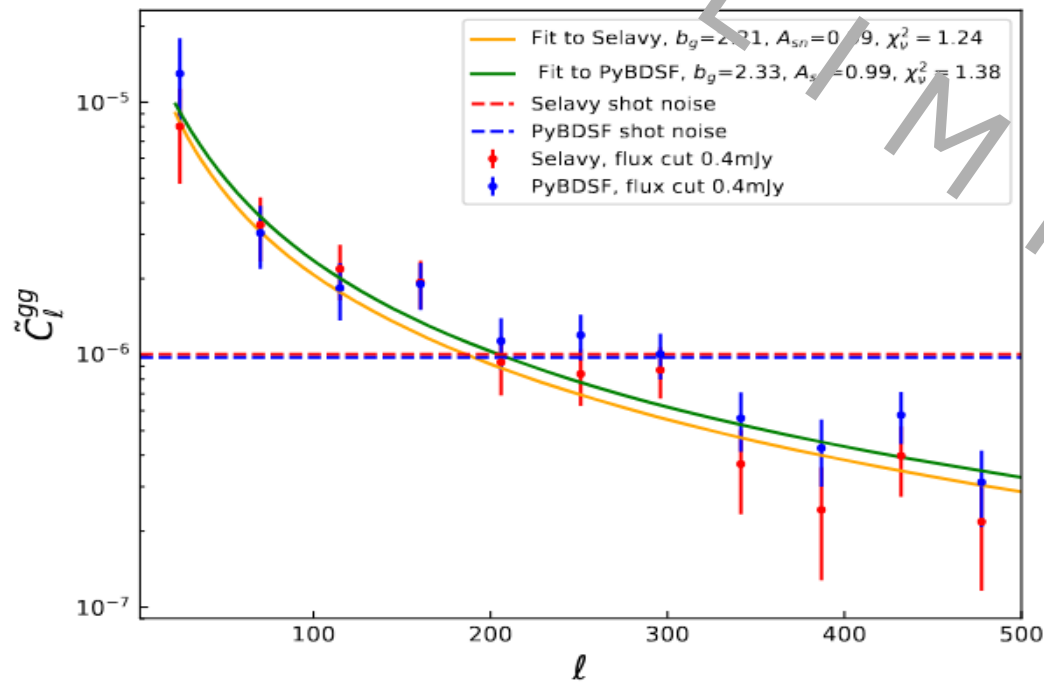
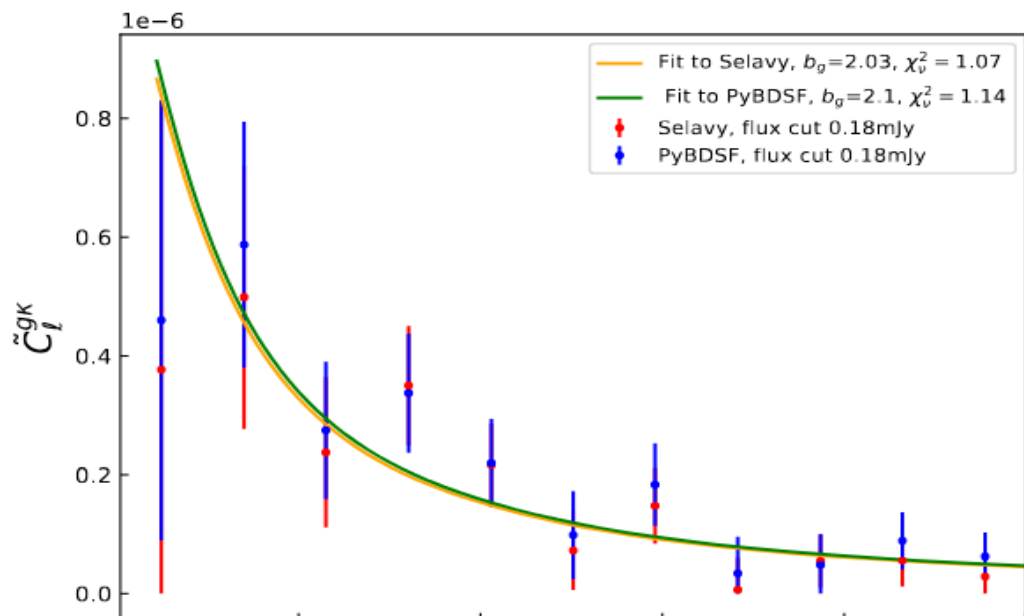
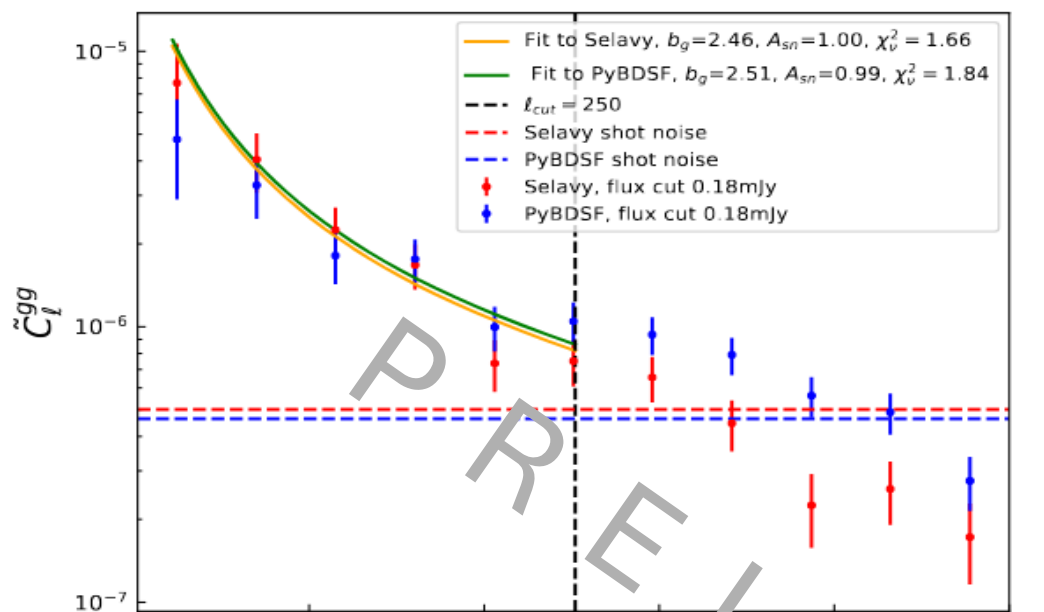
# Methodology

- Assume both a linear and a HALOFIT matter power spectrum
- Consider two different galaxy bias models: a constant bias  $b(z)=b_g$  ; and a constant amplitude  $b(z)=b_g/D(z)$ , with  $D(z)$  the linear growth factor
- Assume the analytic Gaussian covariance in the log-likelihood
- Consider scales from  $l=2$  to 500 (corresponding to  $k_{\max}=0.15 \text{ Mpc}^{-1}$  at  $z\sim 1$ , after which linear galaxy models no longer hold)

# Methodology

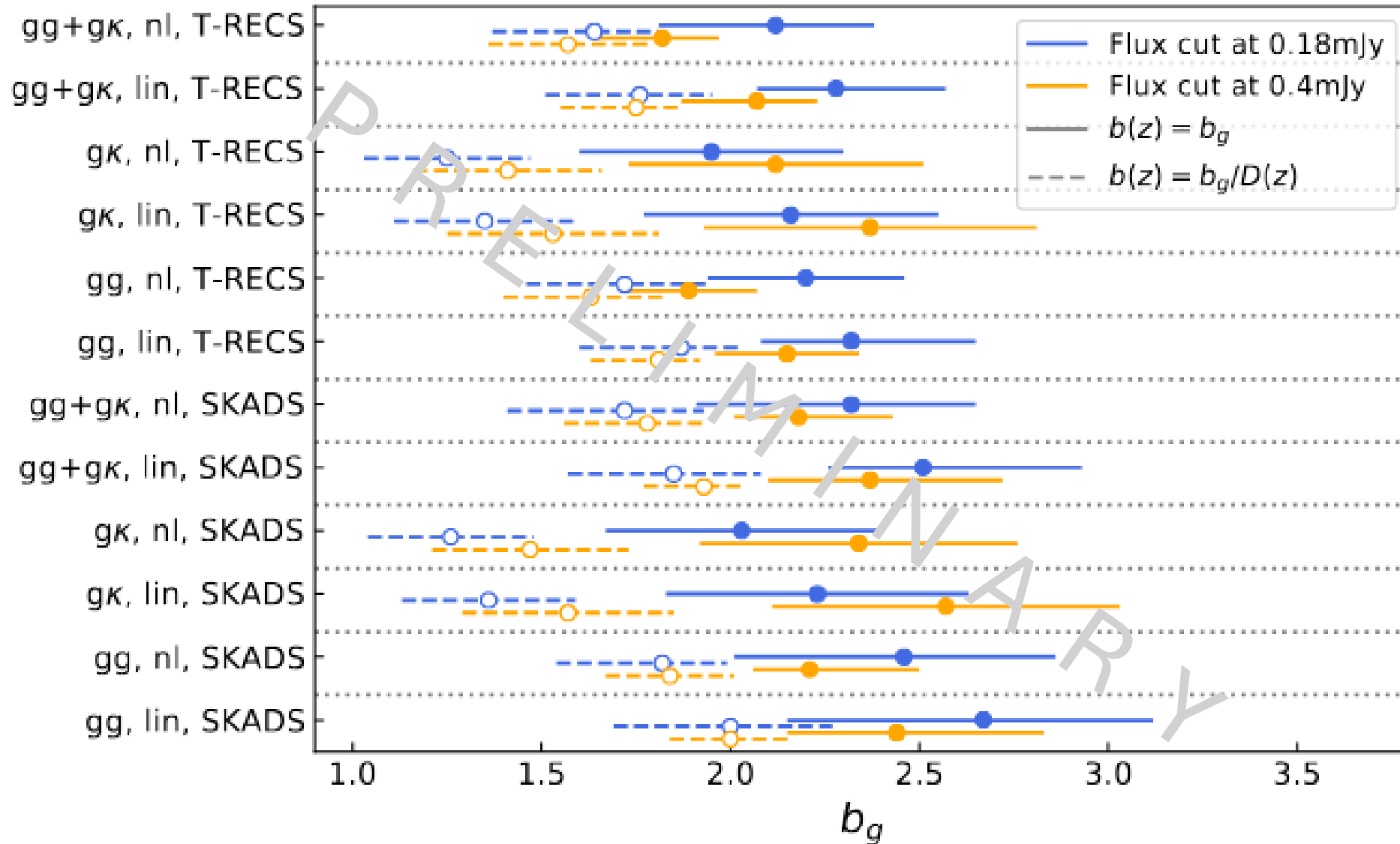
- Assume both a linear and a HALOFIT matter power spectrum
- Consider two different galaxy bias models: a constant bias  $b(z)=b_g$  ; and a constant amplitude  $b(z)=b_g/D(z)$ , with  $D(z)$  the linear growth factor
  - Assume the analytic Gaussian covariance in the log-likelihood
- Consider scales from  $l=2$  to 500 (corresponding to  $k_{\max}=0.15 \text{ Mpc}^{-1}$  at  $z\sim 1$ , after which linear galaxy models no longer hold)
- Add an extra nuisance amplitude parameter to account for deviations from shot noise (contributions from multi-components, halo exclusion, non-local and stochastic effects in galaxy formation)

# Cross-correlation significance $\sim 5.4\sigma$

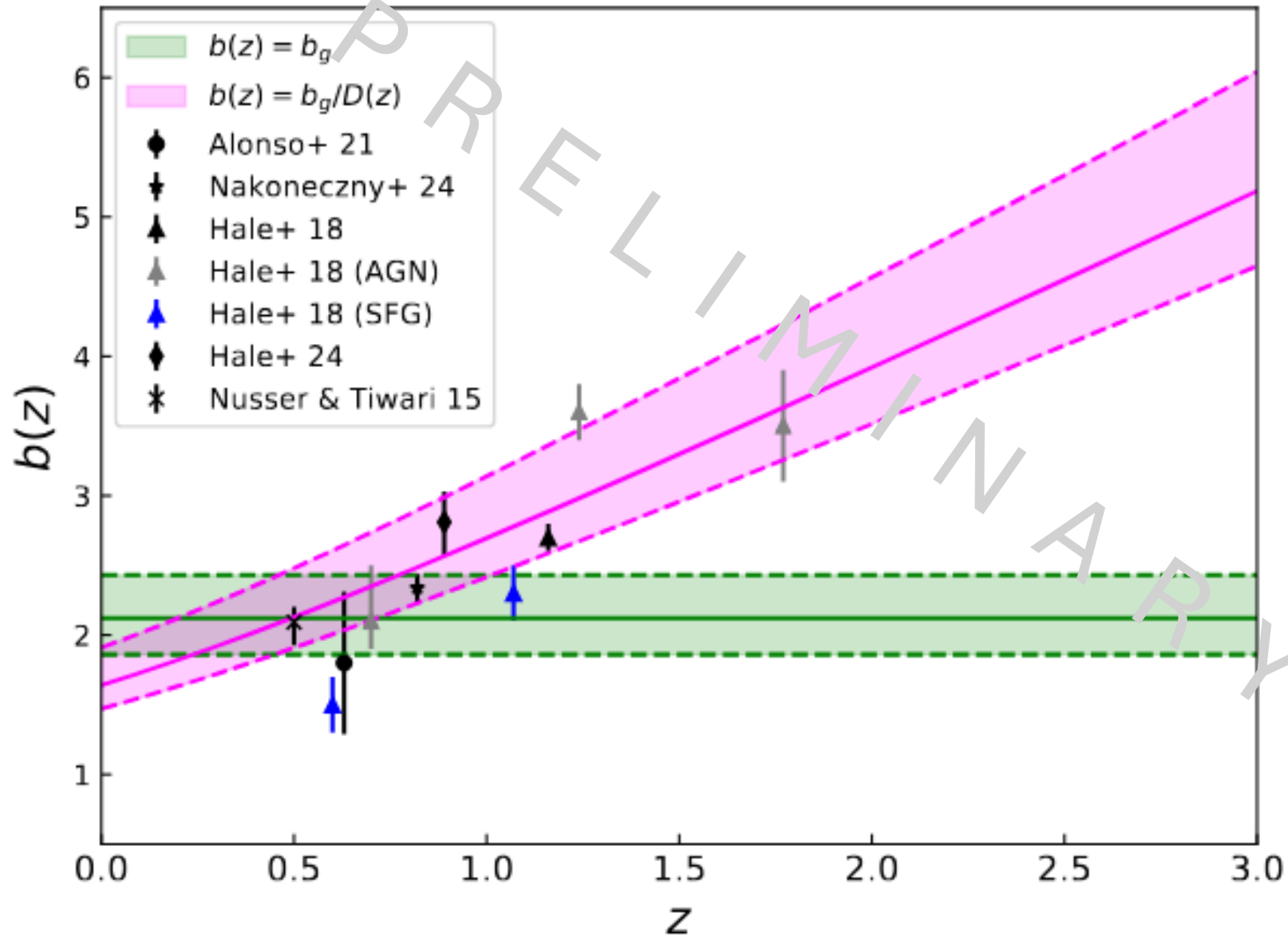




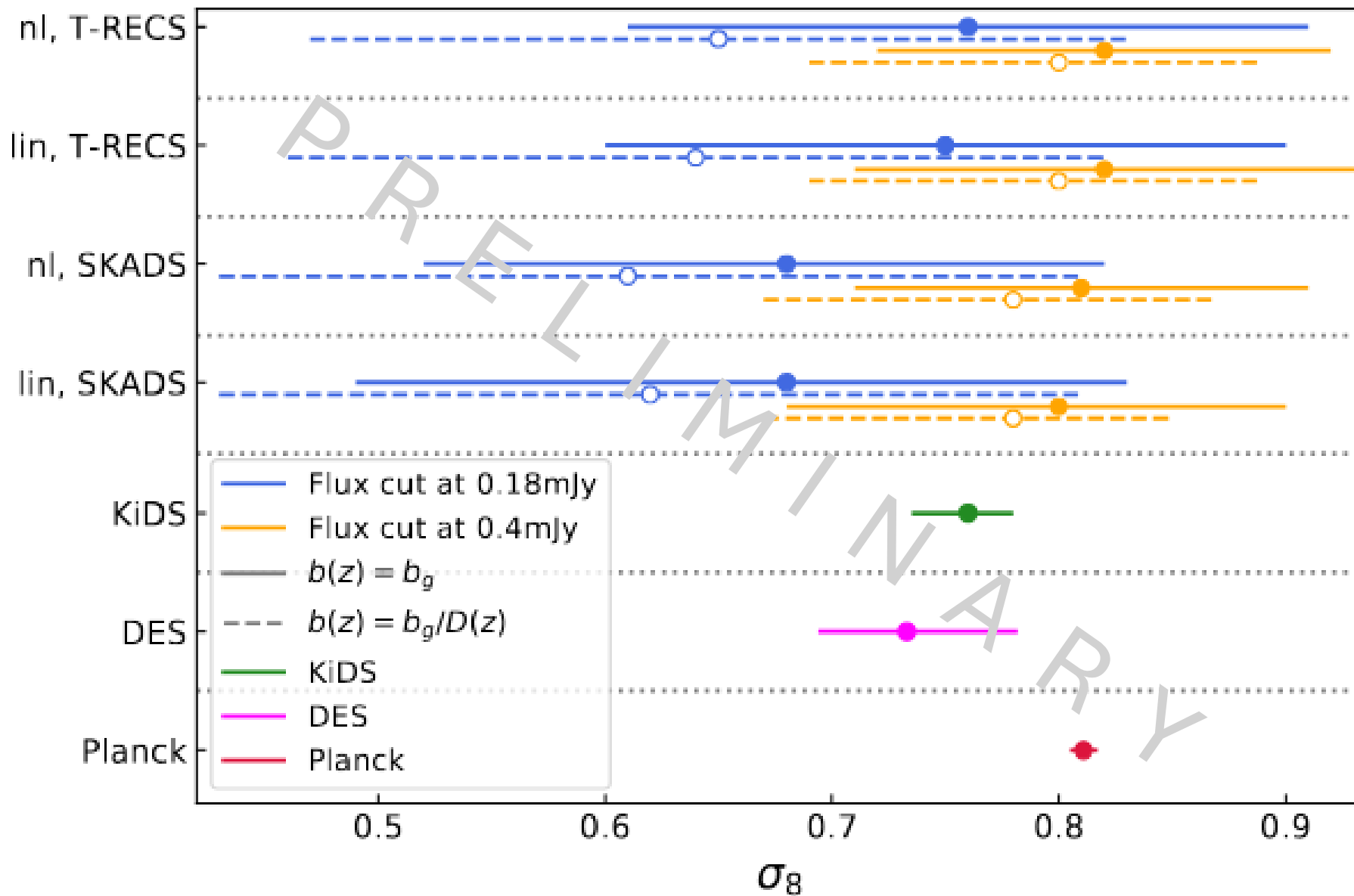
# Galaxy bias constraints (fixed cosmology)



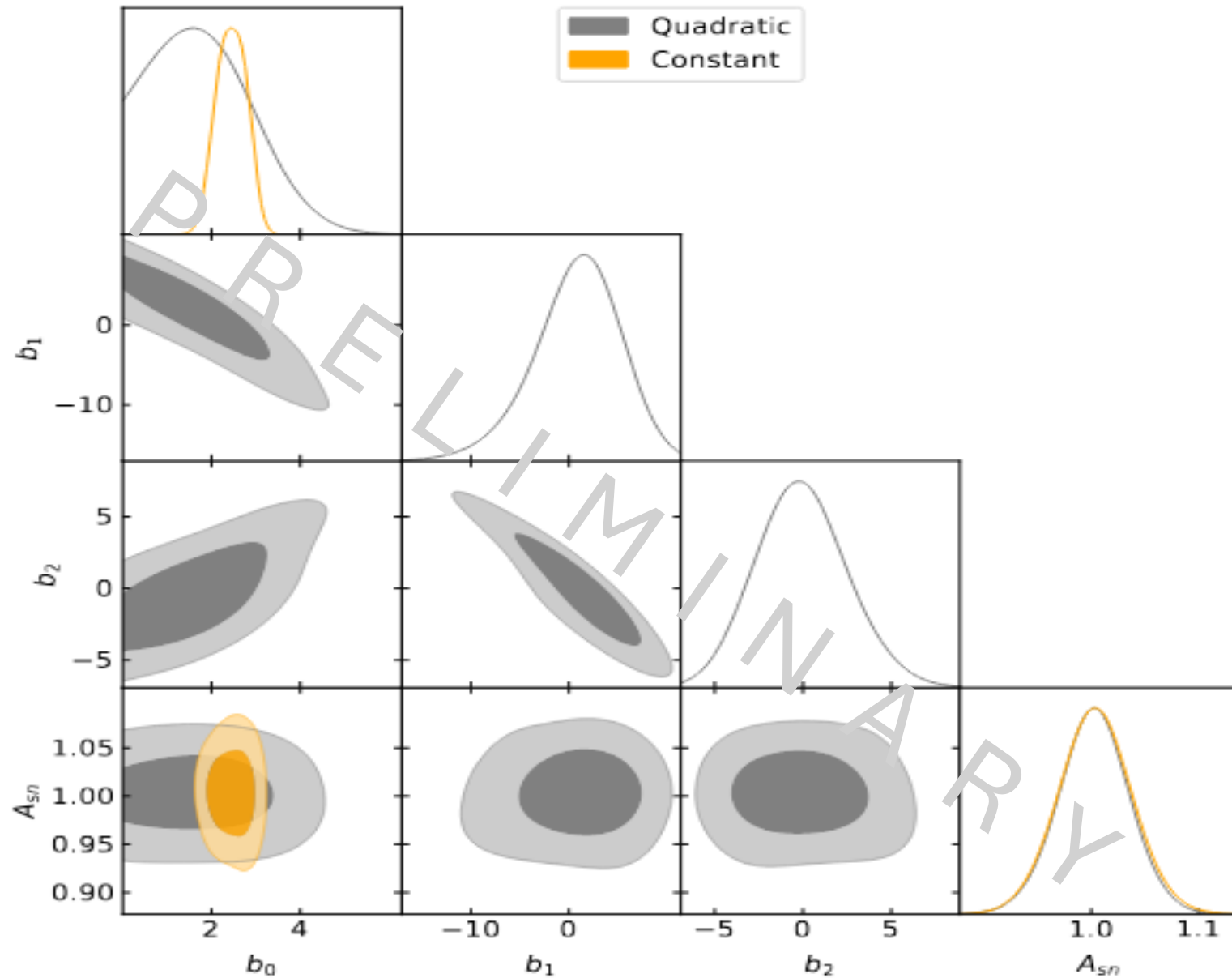
# Galaxy bias constraints (fixed cosmology)



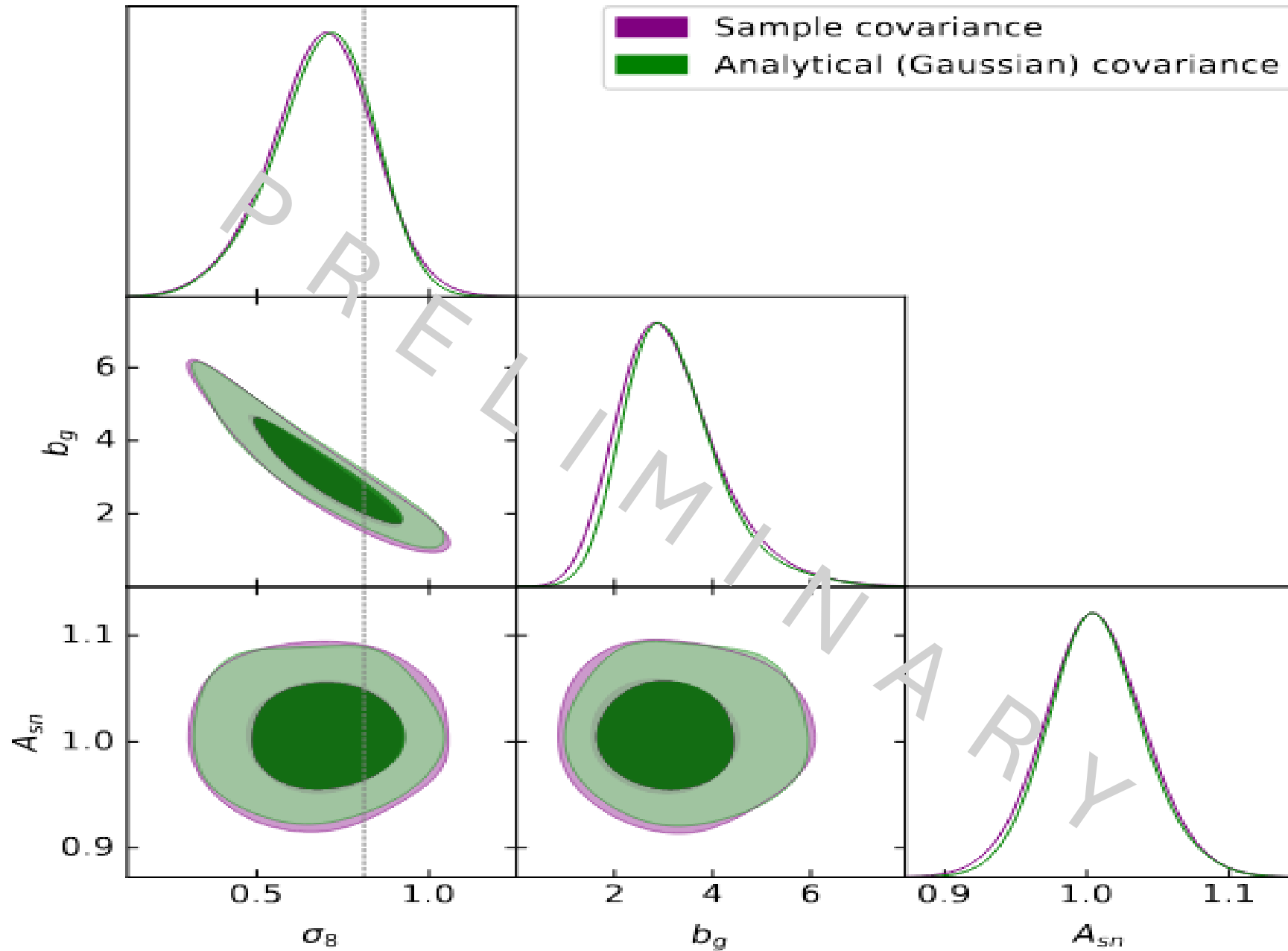
# Cosmology constraints



# Quadratic galaxy bias: $b(z) = b_0 + b_1z + b_2z^2$



# Comparison with numerical covariance



# Conclusions

- Analysed the EMU PSI data using the harmonic-space power spectra
- Considered two catalogues for the measurements, Selavy and PyBDSF, and saw differences after  $l \sim 250$  depending on the flux cut
  - Detected cross-correlation with CMB lensing with  $\text{SNR} \sim 5.4$
- Constrained the galaxy bias and  $\sigma_8$  using different flux cuts, a linear and HALOFIT power spectrum and assuming the SKADS and T-RECS redshift distributions for a constant bias and a constant amplitude model

**Thank you!**

**Back-up slides**



# Numerical covariance using GLASS

$$\text{Cov}_{\ell\ell'}^{WX,YZ} = \frac{1}{N_m - 1} \sum_{m=1}^{N_m} \left( \tilde{C}_\ell^{WX,m} - \langle \tilde{C}_\ell^{WX} \rangle \right) \left( \tilde{C}_\ell^{YZ,m} - \langle \tilde{C}_\ell^{YZ} \rangle \right)$$

$$\langle \tilde{C}_\ell^{WX} \rangle = \frac{1}{N_m} \sum_{m=1}^{N_m} \tilde{C}_\ell^{WX,m}$$

$$\text{Cov}^{-1} \rightarrow \frac{N_m - N_d - 2}{N_m - 2} \text{Cov}^{-1}$$

# 2D corner plots

